Numerical Analysis of Unsteady Vibrations of a Plate Resting on an Elastic Isotropic Half-Space

MARINA V. SHITIKOVA[1,2], ANNA S. BESPALOVA[1]
[1]Research Center on Dynamics of Structures,
Voronezh State Technical University,
20-Letija Oktjabrja Str. 84, Voronezh 394006,
RUSSIA

[2]Department of High Mathematics,
National Research Moscow State University of Civil Engineering,
Yaroslavskoye Shosse 26, Moscow 127238,
RUSSIA

Abstract: - The paper is devoted to the numerical solution of the problem of vibrations of an infinite elastic plate resting on an elastic isotropic half-space using the analytical method based on the ray method with its numerical realization via the Maplesoft package. Unsteady oscillations are caused by the action of instantaneous loads on the plate, resulting in the appearance of two plane wave surfaces of strong discontinuity in the elastic half-space, behind the fronts of which, up to the contact boundary, the solution is constructed using ray series. The unknown functions entering the coefficients of the ray series and the equation of plate motion are determined from the boundary conditions of the contact interaction between the plate and the half-space. Previously, the approximate solution of this problem was obtained analytically without using mathematical packages, and the dynamic deflection of the plate involving only the first three terms of the ray series was written down. In this work, a two-layer medium with different properties was investigated using an algorithm developed to solve contact dynamic problems related to the occurrence and propagation of strong and weak discontinuity surfaces.

Key-Words: - Dynamic contact, infinitely long elastic plate, ray method, truncated ray series, nonstationary vibrations, conditions of compatibility, theory of discontinuities.

Received: April 5, 2023. Revised: December 17, 2023. Accepted: February 11, 2024. Published: April 3, 2024.

1 Introduction

Problems devoted to the analysis of the impact interaction of solids remain relevant to date, as they are widely used in various fields of science and technology, [1], [2], [3], [4], [5]. The physical phenomena involved in the process of impact interaction include dynamic reactions of contacting bodies, effects of contact conditions, and wave propagation. Since such problems belong to the class of problems of dynamic contact interaction, their solution is associated with significant mathematical and computational difficulties, which include not only the complex equations describing the dynamic behavior of a continuous medium but also the variety of boundary conditions on the contacting surfaces of solids, [6], [7], [8], [9], [10], [11].

All dynamic contact problems can be divided into two types. The first type includes the problems related to the propagation of harmonic vibrations and waves (bodies are either in constant contact with each other or in prolonged contact). The second type involves the problems related to the propagation of surfaces of strong or weak discontinuity, as well as the problems leading to unsteady oscillatory motions (short-term contact of bodies, or shock interaction), [1].

To solve the problems of the first and second types, different mathematical methods are used. Among the main methods for solving problems of the second type should be mentioned the following: the method of invariant-functional solutions [3], the Wiener-Hopf method [3], the method of characteristics [12], various numerical methods, and the ray method, [1], [6], [9], based on the theory of geometrical optics and its generalizations.

The ray method is most effective in solving problems of propagation and attenuation of transient

waves carrying jumps of field parameters at the wavefront, [1].

The zero term of the ray series exactly describes the changes in the jump of field parameters along the ray, but the rest of terms within the radius of the series convergence describe the changes in the field behind the wavefront, [1], [6].

The question of application of ray series to the problems of transient wave problems has been considered by many researchers, and yet, until recently, the area of its practical applicability, which is largely determined by the possibility of calculating a sufficient number of coefficients of the ray series. sufficient number of ray series coefficients and the radius of convergence of the ray series, remained poorly studied, [1], [13].

Since in practice one has to limit oneself to finite truncated ray series to construct a solution, instead of the question of convergence, the problem of uniform convergence of the solved truncated ray series in the region of existence of wave motion is most often solved.

All ray series used could be divided into two main groups [1]. The ray series of the first group are mainly used in wave dynamics problems for approximation of physical fields of regular functions. The second type of ray series is used for the approximation of physical fields of singular functions.

The majority of the studies devoted to ray methods based on ray series of both types deal with the volume wave investigation. However, ray methods are also successfully applied to the study of waves propagating along the free surface, waves propagating along the interface between two media, and nonstationary Love waves, [1], [5], [13], [14].

This paper presents a description of an algorithm developed based on the Maplesoft package for solving contact dynamic problems related to the generation and propagation of surfaces of strong and weak discontinuity by an analytical method based on the ray method. Numerical investigations of a two-layer medium with different properties have been performed based on this algorithm.

2 Problem Formulation

The solution of the problem of unsteady vibrations of a plate of constant thickness on an elastic isotropic half-space was constructed in [15], for the case of a sliding contact between the plate and the half-space. The ray method, [1], was used as a method of solution, which allowed one to obtain the time dependence of the plate displacements in an analytical form. In this case, the author of [15], managed to determine only the first three terms of the ray series "manually".

The purpose of this paper is to develop an algorithm based on the Maple software package for solving various contact dynamic problems related to the generation and propagation of strong and weak discontinuity surfaces using the ray method. This approach will make it possible to determine a sufficiently large number of members of the ray series, which, in turn, allows one to obtain a solution with a sufficiently large accuracy.

For this purpose, following [15], let us consider a layer on a foundation, which is modeled by a half-space with x, y, z coordinate system (Figure 1).

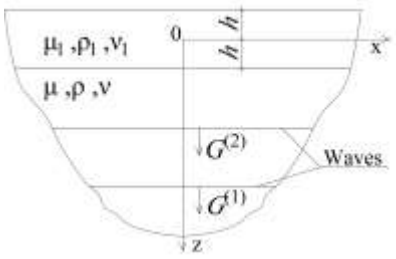

Fig. 1: Calculation scheme

The layer and the supporting half-space are homogeneous, isotropic, and linearly elastic. The plane deformed state is realized, in which the displacement component in the y-axis direction is zero, and the displacements along the x and z-axes are the functions of the x and z coordinates, respectively.

The dynamic behavior of the layer is modeled by a classical plate, the equation of motion of which has the form:

$$\frac{4\mu_1 h^3}{3(1-\nu_1)}\frac{\partial^4 W}{\partial x^4}+2\rho_1 h\frac{\partial^2 W}{\partial t^2}-p=0\,, \qquad (1)$$

where $W(x,\ t)$ is the displacement of the middle plane of the plate (z=0), $2h$ is the plate thickness, μ_1, ν_1 and ρ_1 are shear modulus, Poisson's ratio and density of the plate material, respectively, and $p(x,t)$ is the transverse surface load.

The set of equations describing the dynamic behavior of an isotropic half-space has the form:

$$\frac{\partial \sigma_{ij}}{\partial x_j}=\rho\frac{\partial^2 u_i}{\partial t^2}\,,$$

$$\sigma_{ij}=\lambda\frac{\partial u_k}{\partial x_k}\delta_{ij}+\mu\left(\frac{\partial u_i}{\partial x_j}+\frac{\partial u_j}{\partial x_i}\right) \qquad (2)$$

where σ_{ij} and u_i are the components of the stress tensor and displacement vector, respectively, ρ is the density of the half-space material, λ and μ are

Lame parameters, δ_{ij} is the Kronecker symbol, Latin indices take on values 1 and 3, i.e. $x_1 = x$, and $x_3 = z$.

The plate and the half-space are in contact at $z = h$. For the case of the sliding contact, the boundary conditions could be written as follows:

$$\sigma_{33}(x,h,t) = p(x,t),\ \sigma_{13}(x,z,t) = 0,$$
$$u_3(x,z,t) = W(x,t). \quad (3)$$

Unsteady plate vibrations are excited by sending velocities to the points of the plate at the initial moment of time

$$\left.\frac{\partial W}{\partial t}\right|_{t=0} = c(x), \quad (4)$$

where $c(x)$ is a given function.

3 Method of Solution

As a result of instantaneous action of velocities (4) on the plate, two surfaces of strong discontinuity (volume waves of compression and shear) appear in the half-space, behind the fronts of which the solution for desired functions is constructed in the form of the ray series, [1], [9]

$$Z(x,z,t) = \sum_{k=0}^{\infty} \frac{1}{k!}\left[Z_{,(k)}\right]\left(t-\frac{z-h}{G}\right)^k H\left(t-\frac{z-h}{G}\right) \quad (5)$$

where $\left[Z_{,(k)}\right] = [\partial^k Z/\partial t^k]$ are jumps in the k-th order time derivatives of the functions Z on the shock wave fronts $\sum$, i.e. at $t=(z-h)/G$, $H(t)$ is the unit Heaviside function, and G is the shock wave velocity.

To determine the coefficients of the ray series (5), it is necessary to differentiate the first equation in (2) k times and the second equation $k+1$ times in time, write down their difference on different sides of the wave surface and apply the conditions of compatibility, [1], for jumps of $k+1$ derivatives of the functions $Z(x, z, t)$:

$$G\left[\frac{\partial Z_{,(k)}}{\partial x_i}\right] = -\left[Z_{,(k+1)}\right]\nu_i + \frac{d\left\lfloor Z_{,(k)}\right\rfloor}{dt}\nu_i + G\frac{\partial\left[Z_{,(k)}\right]}{\partial x_1}\delta_{i1}, \quad (6)$$

where ν_i are the components of the unit normal vector to the wave surface, δ_{i1} is the Kronecker symbol, and d/dt is the Thomas delta-derivative, [16].

As a result, the following set of recurrence equations is obtained:

$$\left[\rho G^2 - (\lambda+2\mu)\right]\omega_{(k+1)} = -2(\lambda+2\mu)\frac{d\omega_{(k)}}{dt} - (\lambda+\mu)G\frac{\partial w_{(k)}}{\partial x} - F_{(k-1)}, \quad (7)$$

$$\left(\rho G^2 - \mu\right)w_{(k+1)} = -2\mu\frac{dw_{(k)}}{dt} - (\lambda+\mu)G\frac{\partial\omega_k}{\partial x} - \Phi_{(k-1)}, \quad (8)$$

where $\omega_{(k)} = \left[\nu_{i,(k)}\right]\nu_i$, $w_{(k)} = \left[\nu_{i,(k)}\right]\delta_{i1}$, $\nu_i = u_{i,(1)}$,

$$F_{(k-1)} = -(\lambda+2\mu)\frac{d^2\omega_{(k-1)}}{dt^2} - \mu G^2\frac{d^2\omega_{(k-1)}}{dx^2} - G(\lambda+\mu)\frac{d}{dt}\left(\frac{\partial w_{(k-1)}}{\partial x}\right),$$

$$\Phi_{(k-1)} = -\mu\frac{d^2 w_{(k-1)}}{dt^2} - (\lambda+2\mu)G^2\frac{d^2 w_{(k-1)}}{dx^2} - G(\lambda+\mu)\frac{d}{dt}\left(\frac{\partial\omega_{(k-1)}}{\partial x}\right).$$

Solution of the recurrence equations (7) - (8) at k = -1,0,1,2... results in the expressions for determining the velocity of the first wave $\rho G^{(1)^2} = (\lambda+2\mu)$ and the second wave $\rho G^{(2)^2} = \mu$, as well as the values of $\omega_{(k)}$ and $w_{(k)}$ on the both waves up to arbitrary functions, where the upper index in parentheses denotes the ordinal number of the wave, and the lower index in parentheses denotes the ordinal number of the jump.

Since in this paper, unlike [13], mathematical calculations for finding these quantities are carried out using the Maple computer algebra system, no restrictions are imposed on the number of defined members of the ray series.

The solution is reduced to integration of the differential equations of motion of the medium (7)-(8) subjected to the initial conditions at each wave.

Thus, on the first wave

$$w^{(1)}_{(-1)} = 0,\ \omega^{(1)}_{(-1)} = 0,\ w^{(1)}_{(0)} = 0,\ \omega^{(1)}_{(0)} = f_0(x) \quad (9)$$

Next, a loop is written to determine the N values of $\omega_{(k)}$ and $w_{(k)}$ on the first wave:

for i **from** 1 **to** N **do**

$$w^{(1)}_{(i)} = \frac{1}{\rho G^{(1)^2} - \mu}\left[-2\mu\frac{dw^{(1)}_{(i-1)}}{dt} - (\lambda+\mu)G^{(1)}\frac{\partial\omega^{(1)}_{(i-1)}}{\partial x} + \mu\frac{d^2 w^{(1)}_{(i-2)}}{dt^2} + (\lambda+2\mu)G^{(1)^2}\frac{d^2 w^{(1)}_{(i-2)}}{dx^2} + (\lambda+\mu)G^{(1)}\frac{d}{dt}\left(\frac{\partial\omega^{(1)}_{(i-2)}}{\partial x}\right)\right],$$

$$\omega_{(i)}^{(1)}=\frac{1}{2(\lambda+2\mu)}\int\Bigg[-(\lambda+\mu)G^{(1)}\frac{\partial w_{(i)}^{(1)}}{\partial x}+(\lambda+2\mu)\frac{d^2\omega_{(i-1)}^{(1)}}{dt^2}$$

$$+\mu G^{(1)^2}\frac{d^2\omega_{(i-1)}^{(1)}}{dx^2}+(\lambda+\mu)G^{(1)}\frac{d}{dt}\left(\frac{\partial w_{(i-1)}^{(1)}}{\partial x}\right)\Bigg]dt+f_i(x);$$

end do

Similar actions are performed on the second wave:

$$w_{(-1)}^{(2)}=0,\ \omega_{(-1)}^{(2)}=0,\ w_{(0)}^{(2)}=0,\ \omega_{(0)}^{(2)}=g_0(x) \quad (10)$$

for i **from** 1 **to** N **do**

$$\omega_{(i)}^{(2)}=\frac{1}{\rho G^{(2)^2}-(\lambda+2\mu)}\Bigg[-2(\lambda+2\mu)\frac{d\omega_{(i-1)}^{(2)}}{dt}$$

$$-(\lambda+\mu)G^{(2)}\frac{\partial w_{(i-1)}^{(2)}}{\partial x}+(\lambda+2\mu)\frac{d^2\omega_{(i-2)}^{(2)}}{dt^2}+\mu G^{(2)^2}\frac{d^2\omega_{(i-2)}^{(2)}}{dx^2}$$

$$+(\lambda+\mu)G^{(2)}\frac{d}{dt}\left(\frac{\partial w_{(i-2)}^{(2)}}{\partial x}\right)\Bigg];$$

$$w_{(i)}^{(2)}=\frac{1}{2\mu}\int\Bigg[-(\lambda+\mu)G^{(2)}\frac{\partial\omega_{(i)}^{(2)}}{\partial x}+\mu\frac{d^2w_{(i-1)}^{(2)}}{dt^2}$$

$$+(\lambda+2\mu)G^{(2)^2}\frac{d^2w_{(i-1)}^{(2)}}{dx^2}+(\lambda+\mu)G^{(2)}\frac{d}{dt}\left(\frac{\partial\omega_{(i-1)}^{(2)}}{\partial x}\right)\Bigg]dt$$

$$+g_i(x);$$

end do

As it is known, [6], [12], behind the front of the strong discontinuity surface, the solution for the desired function is constructed in the form of a ray series (5), wherein the jumps of the k-th order time-derivatives of the function Z on the wave surface are calculated at $t=(z-h)/G$. Therefore, the next action for each of the defined quantities $\omega_{(k)}$ and $w_{(k)}$ is to replace the parameter t by $t=(z-h)/G$.

The obtained jumps allow one to define the desired functions u_1 and u_3 for the half-space in the form of truncated ray series

$$u_1=\sum_{\alpha=1}^{2}\sum_{k=1}^{N}\frac{1}{k!}\left(t-\frac{z-h}{G^{(\alpha)}}\right)^k w_{(k-1)}^{(\alpha)}\Bigg|_{t=(z-h)/G^{(\alpha)}}H\left(t-\frac{z-h}{G^{(\alpha)}}\right) \quad (11)$$

$$u_3=\sum_{\alpha=1}^{2}\sum_{k=1}^{N}\frac{1}{k!}\left(t-\frac{z-h}{G^{(\alpha)}}\right)^k \omega_{(k-1)}^{(\alpha)}\Bigg|_{t=(z-h)/G^{(\alpha)}}H\left(t-\frac{z-h}{G^{(\alpha)}}\right) \quad (12)$$

where N is the number of considered terms in the ray expansion.

To construct the solution for the plate, the ray series (11) and (12) and the ray expansions for the stresses σ_{13} and σ_{33} should be written at the contact boundary:

$$u_3=u_3\big|_{z=h},\ u_1=u_1\big|_{z=h},\ \sigma_{13}=\sigma_{13}\big|_{z=h},\ \sigma_{33}=\sigma_{33}\big|_{z=h} \quad (13)$$

At the next stage, the obtained solutions are spliced together on the contact boundary. For this purpose, the contact conditions (3), the initial condition (4) and the equation of motion of the plate (1) should be considered. The values involved in equation (1) are written as follows:

$$W=\sum_{k=1}^{N}\frac{1}{k!}W_{(k)}t^k,\ \ p=\sum_{k=1}^{N}\frac{1}{k!}p_{(k)}t^k \quad (14)$$

Substituting relationships (11) and (12) into the above equations and equating the coefficients at the same orders of t, arbitrary functions $f_{(a)}(x)$, $g_{(a)}(x)$, $(a=0,1,2,3...)$ are determined at each step, as well as the required values $W_{(k)}$ and $p_{(k)}$. Then, taking the obtained values into account and considering (14), the ray series could be constructed to determine the displacement of the plate and the reaction force of the half-space.

4 Numerical Results

To carry out numerical investigations, let us assume for certainty that

$$c(x)=W_0\cos\frac{lx}{h}, \quad (15)$$

where W_0 and l are some constants.

Then, the four-term truncated ray series for W will take the form:

$$W=\Bigg\{t-\frac{\rho G^{(1)}}{2\rho_1 h}\frac{t^2}{2}+\left[\left(\frac{\rho G^{(1)}}{2\rho_1 h}\right)^2-\frac{2l^4\mu_1}{3\rho_1(1-\nu_1)h^2}\right]\frac{t^3}{6}$$

$$+\Bigg[-\left(\frac{\rho G^{(1)}}{2\rho_1 h}\right)^3++\frac{2l^4\mu_1\rho G^{(1)}}{3\rho_1^2(1-\nu_1)h^3}+\frac{l^2\rho}{2\rho_1 h^3}\Big(4G^{(2)^3} \quad (16)$$

$$-4G^{(1)}G^{(2)^2}+\frac{1}{2}G^{(1)^3}\Big)\Bigg]\frac{t^4}{6}\Bigg\}W_0\cos\frac{l}{h}x.$$

The main attention in studies of unsteady vibrations of a plate is paid to its dynamic displacement, because this value is important for practice. For this purpose, it is more convenient to rewrite the resulting expression for the displacement in the dimensionless form W^* using the following relations:

$$W^* = \frac{G^{(1)}}{h}\frac{W}{W_0},\ t^* = t\frac{G^{(1)}}{h},\ \rho^* = \frac{\rho_1}{\rho},\ \mu^* = \frac{\mu_1}{\mu},$$
$$x^* = \frac{x}{h},\ G^* = \frac{G^{(2)}}{G^{(1)}}. \quad (17)$$

We will study a two-layer medium with the following constant parameter values: $\cos(lx^*)=1$, $l=1$, $\nu_1 = 0.2$, $\nu = 0.37$. The results for four examples will be evaluated in terms of amplitude and period depending on different values of dimensionless quantities of ρ^* and μ^*.

First example. Let us consider the first variant of the two-layered medium: the plate is light and rigid with $\rho^* = 0.82$ and $\mu^* = 557.36$ (the choosing ratios of parameters correspond to light concrete and loam soil with porosity coefficient $e=0.45$).

The results of calculations obtained with the developed algorithm based on the Maplesoft considering different number of terms in the ray expansion are shown in Figure 2 for $N = 4 – 22, 25, 30$.

To estimate the amplitude and period of oscillations during dynamic contact interaction, characteristic time points were determined, namely: values of t^* at which the dimensionless deflection W^* attains its maximal and minimal magnitudes, i.e. extrema of the function W^*, and magnitudes of t^* corresponding to odd and even half-periods, i.e. when $W^*=0$ (data are given in Table 1, Table 2, Table 3 and Table 4 for the first and third examples).

It is seen from Figure 2 that the curves plotted for a large number of members of the series almost coincide and repeat the trajectory, indicating the convergence of the solution with the increase in the number of terms of the ray series.

Having analyzed the data from Table 1, we could draw a conclusion that the difference in the values of t^* when dynamic deflection attains its extremum magnitude $W^*=W^*_{max}$ calculated at $N=4$ (the number of terms used in the "manual" calculation) and at $N=7$ is around 10%, while for the first half-period, i.e. when $W^*=0$, the difference is 19.5%. It could be also seen from Figure 2 that the period of oscillation is approximately around the value of $t^*=0.6$. So, if we are interested in the period of oscillation, it is necessary to determine 14 or 16 terms of the ray series. If we need to advance in time, it is worth using the expansion in terms of a 30-term truncated ray series for a more reliable picture. And if the task is to determine the maximum displacement, to find the maximum stresses to check the local strength, then in principle it is sufficient to restrict oneself by 4 terms of the ray expansion or to determine 5 terms for a more accurate value.

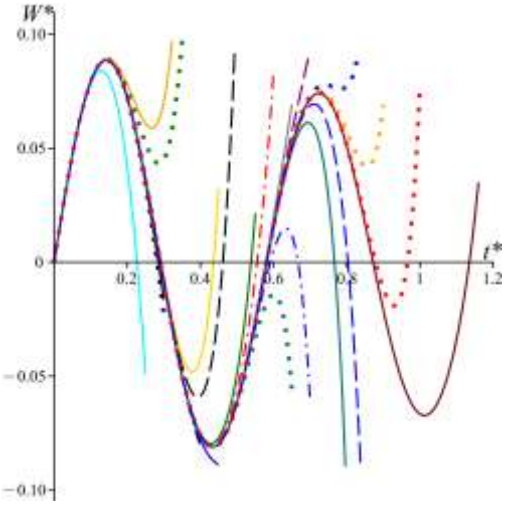

Fig. 2: The dimensionless time t^* dependence of the dimensionless deflection W^* for the first example at different numbers of the ray expansion terms:

-N=4 -N=15
-N=5 -N=16
-N=6 -N=17
-N=7 -N=18
-N=8 -N=19
-N=9 -N=20
-N=10 -N=21
-N=11 -N=22
-N=12 -N=25
-N=13 -N=30
-N=14

Table 1. Magnitudes of time t^* at which the oscillation amplitude attains its extreme values for the first example according to Figure 2

Number of terms of the series	The t^* value for $W^*=W^*_{extr}$ Ordinal number of extremum 1	2	3	4	
N=4	0.129	-	-	-	
N=5	0.146	0.267	-	-	
N=6	0.144	0.287	-	-	
N=7	0.143	-	-	-	
N=8	0.143	-	-	-	
N=9	0.143	0.378	-	-	
N=10	0.143	0.393	-	-	
N=11	0.143	-	-	-	
N=12	0.143	-	-	-	
N=13	0.143	0.429	-	-	
N=14	0.143	0.431	-	-	
N=15	0.143	0.434	0.601	-	
N=16	0.143	0.434	0.634	-	
N=17	0.143	0.433	-	-	
N=18	0.143	0.433	-	-	
N=19	0.143	0.433	0.694	-	
N=20	0.143	0.433	0.711	-	
N=21	0.143	0.433	0.741	0.785	
N=22	0.143	0.433	0.727	0.856	
N=25	0.143	0.433	0.724	0.929	

N=30	0.143	0.433	0.724	1.013	

The second example: the plate (layer) and the base have the same density, i.e. $\rho^* = 1$, and the plate is rigid, i.e. $\mu^* = 665.24$. The results of calculations considering different number of terms in the ray expansion are shown in Figure 3 for $N = 4 – 22, 25, 30$.

Table 2. Summary table of half-periods for the first example

Number of terms of the series	The t^* value at $W^*=0$ Ordinal number of the half-period 1	2	3	4	
N=4	0.227	-	-	-	
N=5	-	-	-	-	
N=6	-	-	-	-	
N=7	0.282	-	-	-	
N=8	0.285	-	-	-	
N=9	0.292	0.436	-	-	
N=10	0.291	0.461	-	-	
N=11	0.291	-	-	-	
N=12	0.291	-	-	-	
N=13	0.291	0.538	-	-	
N=14	0.291	0.555	-	-	
N=15	0.291	-	-	-	
N=16	0.291	0.591	0.667	-	
N=17	0.291	0.579	-	-	
N=18	0.291	0.581	-	-	
N=19	0.291	0.582	0.767	-	
N=20	0.291	0.581	0.803	-	
N=21	0.291	0.581	-	-	
N=22	0.291	0.581	-	-	
N=25	0.291	0.581	0.879	0.966	
N=30	0.291	0.581	0.872	1.135	

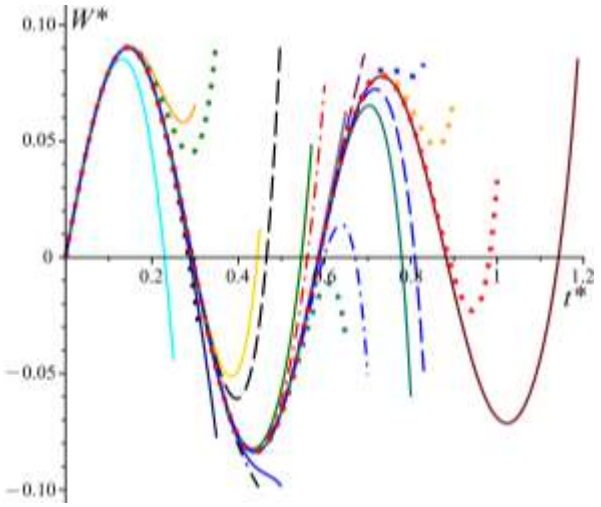

Fig. 3: The dimensionless time t^* dependence of the dimensionless deflection W^* at different numbers of the ray expansion terms (designations are the same as in Figure 2)

The third example: heavy rigid plate with $\rho^* = 1.43$ and $\mu^* = 1168.66$ (these ratios of parameters correspond to heavy concrete and loam soil with porosity coefficient e=0.45). The results of calculations considering different number of terms in the ray expansion are shown in Figure 4 for $N = 4 – 22, 25, 30$. A summary table of t^* values at which the oscillation amplitude attains its extremes and half-period values are compiled in Table 3 and Table 4, respectively.

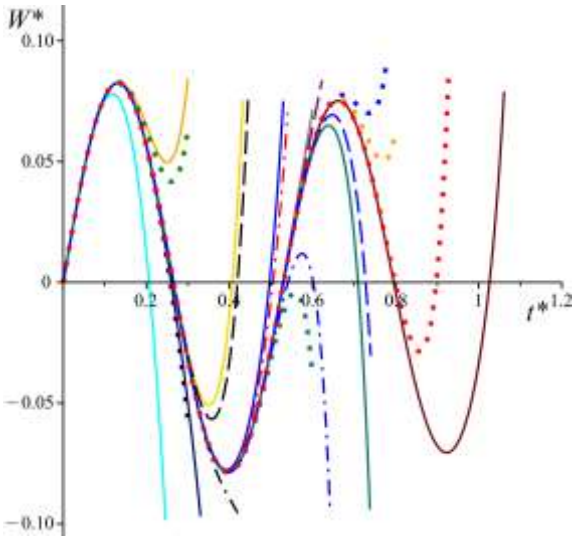

Fig. 4: The dimensionless time t^* dependence of dimensionless deflection W^* for the third example at different numbers of the ray expansion terms (designations are the same as in Figure 2)

Table 3. Time t^* values at which the oscillation amplitude attains its extremes for the third example

Number of terms of the series	The t^* value at $W^*=W^*_{extr}$ Ordinal number of extremum 1	2	3	4	
N=4	0.118	-	-	-	
N=5	0.134	0.251	-	-	
N=6	0.133	0.260	-	-	
N=7	0.131	-	-	-	
N=8	0.131	-	-	-	
N=9	0.131	0.350	-	-	
N=10	0.131	0.358	-	-	
N=11	0.131	-	-	-	
N=12	0.131	-	-	-	
N=13	0.131	0.393	-	-	
N=14	0.131	0.394	-	-	
N=15	0.131	0.397	0.558	-	
N=16	0.131	0.397	0.575	-	
N=17	0.131	0.396	-	-	
N=18	0.131	0.396	-	-	
N=19	0.131	0.396	0.639	-	
N=20	0.131	0.396	0.647	-	
N=21	0.131	0.396	0.670	0.737	
N=22	0.131	0.396	0.665	0.770	
N=25	0.131	0.396	0.661	0.858	
N=30	0.131	0.396	0.661	0.923	

Table 4. Summary table of half-period values for the third example

Number of terms of the series	The t^* value at $W^*=0$ Ordinal number of the half-period 1	2	3	4	
N=4	0.207	-	-	-	
N=5	-	-	-	-	
N=6	-	-	-	-	
N=7	0.258	-	-	-	
N=8	0.260	-	-	-	
N=9	0.266	0.407	-	-	
N=10	0.265	0.419	-	-	
N=11	0.265	-	-	-	
N=12	0.265	-	-	-	
N=13	0.265	0.497	-	-	
N=14	0.265	0.505	-	-	
N=15	0.265	-	-	-	
N=16	0.265	0.541	0.602	-	
N=17	0.265	0.528	-	-	
N=18	0.265	0.529	-	-	
N=19	0.265	0.530	0.709	-	
N=20	0.265	0.530	0.728	-	
N=21	0.265	0.530	-	-	
N=22	0.265	0.530	-	-	
N=25	0.265	0.530	0.799	0.898	
N=30	0.265	0.530	0.795	1.026	

Analyzing the data, as before, we obtain differences in amplitude of 10% and in period of 20%.

The fourth example: very heavy and rigid plate with $\rho^* = 2.35$ and $\mu^* = 1546.23$ (these ratios of parameters correspond to extra heavy concrete and loam soil with porosity coefficient e=0.45). The results of calculations considering different number of terms in the ray expansion are shown in Figure 5 for $N = 4 – 22, 25, 30$.

Analyzing the results obtained above, it could be concluded that the smaller the number of members of the series, the greater the difference in the results when estimating the period. However, reliable results when estimating the amplitude are obtained starting from N=4. Reference to Figure 6 shows that for a rigid plate the dynamic deflection is practically insensitive to its weight if calculated with the same number of ray series terms.

Analyzing the obtained maximum deflection values for the four examples, it could be concluded that the difference between magnitudes calculated at N=4 (manual counting) and N=5 (members of the series determined with the help of mathematical software) is 6%. Therefore, this is sufficient to determine the strength of the structure.

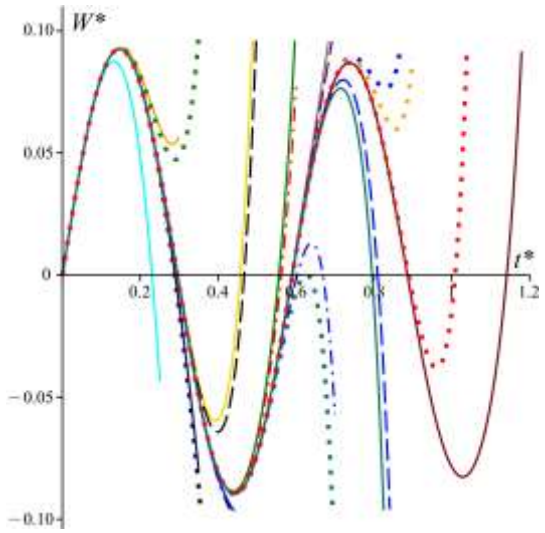

Fig. 5: The dimensionless time t^* dependence of dimensionless deflection W^* at different numbers of the ray expansion terms for the fourth example (designations are the same as in Figure 2)

Maximum magnitudes of the deflection for all four examples within the first half-wave are summarized in Table 5, reference to which shows that it is sufficient to restrict calculations by four-term expansions, i.e. via ‘manual’ calculations.

Table 5. Values of maximum deflection within the first half-wave.

Number of terms of the series	ρ^*=0.82 μ^*= 557.36	ρ^*=1 μ^*= 665.24	ρ^*=1.43 μ^*= 1168.66	ρ^*=2.35 μ^*= 1546.23
N=4	0.084	0.085	0.078	0.087
N=5	0.089	0.091	0.083	0.093
N=6	0.089	0.091	0.083	0.093
N=7	0.089	0.091	0.082	0.093
N=8	0.089	0.091	0.082	0.093
N=9	0.089	0.091	0.082	0.093
N=10	0.089	0.091	0.082	0.093
N=15	0.089	0.091	0.082	0.093
N=16	0.089	0.091	0.082	0.093
N=20	0.089	0.091	0.082	0.093
N=25	0.089	0.091	0.082	0.093
N=30	0.089	0.091	0.082	0.093

5 Conclusion

This paper describes an algorithm developed based on the Maple software package for solving contact dynamic problems related to the generation and propagation of strong and weak discontinuity surfaces using an analytical approach based on the ray method. The efficiency of the constructed algorithm is illustrated on the example of solving the problem of unsteady vibrations of an elastic plate lying on an elastic isotropic half-space, caused

by the action of instantaneous loads on the plate, resulting in the generation and propagation of two plane wave surfaces of strong discontinuity in the elastic half-space. Behind the wave fronts up to the contact boundary, the solution is constructed by means of the ray series. The algorithm for solving such a problem is presented by a program code written in the programming language embedded in the system.

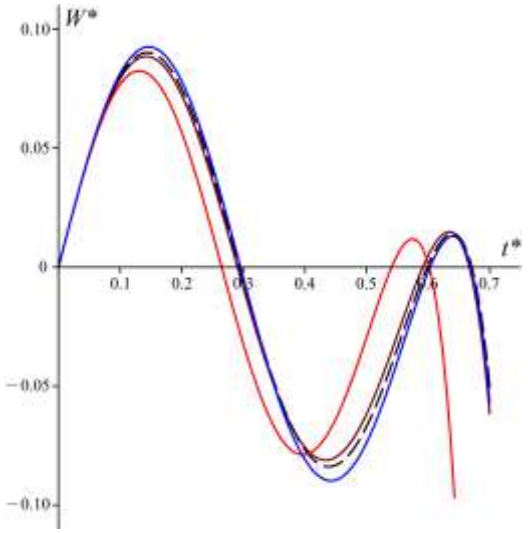

Fig. 6: The dimensionless time t^* dependence of dimensionless deflection W^* at N=16 and different values of ρ^* and μ^*:
- $\rho^* = 0.82$, $\mu^* = 557.36$
- $\rho^* = 1$, $\mu^* = 665.24$
- $\rho^* = 1.43$, $\mu^* = 1168.66$
- $\rho^* = 2.35$, $\mu^* = 1546.23$

Numerical studies have shown that the Maple software package allows one to solve quite complex mathematical and engineering problems. In the considered examples, it is possible to obtain a solution for a significant number of terms of the ray series, which was previously not possible with "manual" calculation, and to demonstrate the convergence of the solution with the increase in the number of terms of the series, as well as to analyze the values of amplitude and period for a two-layer medium with different combinations of properties. It has been established that to determine the period of nonstationary vibrations, it is needed to consider rather large number of terms of the series. To determine the maximum amplitude, in principle, four terms are sufficient, but if the task is to analyze the behavior of the system considering the time progression, a series with 30 terms is optimal.

The developed algorithm could be applied to other types of boundary and initial conditions, as well as it could be generalized for the analysis of dynamic contact interaction for more complex dynamical systems.

Acknowledgement:
The authors thank Mr K.A. Modestov for his consultations concerning the application of the Maple software package.

References:

[1] Yu.A. Rossikhin & M.V. Shitikova, Ray method for solving dynamic problems connected with propagation of wave surfaces of strong and weak discontinuities, *Applied Mechanics Reviews,* Vol. 48, No 1, 1995, pp. 1-39.

[2] I. Colombaro, A. Giusti, & F. Mainardi, On transient waves in linear viscoelasticity, *Wave Motion*, Vol. 74, 2017, pp. 191–212, DOI: 10.1016/j.wavemoti.2017.07.008

[3] V.B. Porutchikov, *Methods of Dynamic Theory of Elasticity* [in Russian], Nauka, Moscow, 1986.

[4] W. Goldsmith, *Impact. The Theory and Physical Behaviour of Colliding Bodies*, Dover Publications, New York, 2001.

[5] J.D. Achenbach, *Wave Propagation in Elastic Solids*, North-Holland Series in Applied Mathematics and Mechanics, Elsevier, 1973.

[6] A.S. Alekseev & B.Ya. Gelchinskiy, Ray method for calculation of head wave intensities, *Questions of Dynamic Theory of Seismic Wave Propagation*, Vol. 5, 1961, pp. 54-72.

[7] J. D. Achenbach & S. P. Keshava, Free waves in a plate supported by a semi-infinite continuum, *Transactions of the American Society of Mechanical Engineers, Journal of Applied Mechanics,* Vol. 34, 1967, pp. 397-404.

[8] J.D. Achenbach, S.P. Keshava, & G. Herrmann, Waves in a smoothly joined plate and half-space, *Journal of the Engineering Mechanics Division, Proceedings of the American Society of Civil Engineers,* Vol. 92, 1966, pp. 113-129.

[9] J.D. Achenbach & D.P. Reddy, Note on wave propagation in linearly viscoelastic media, *Zeitchtift für Angewandte Mathematik und Physik,* Vol. 18, 1967, pp. 141-144.

[10] A.G. Gorshkov & D.V. Tarlakovskii, Resulting reactions in a transient contact problem for an elastic anisotropic half-space,

Journal of Applied Mathematics and Mechanics, Vol. 60, issue 5, 1996, pp. 799-809.

[11] P.V. Kzauklis & L.A. Molotkov, About low-frequency vibration of a plate on an elastic half-space, *Soviet Applied Mechanics*, Vol. 27, 1963, pp. 947-951.

[12] M. Mochihara & Y. Tanaka, Behavior of plates in the elastic range under transverse impact, *Research Reports of Kagoshima Technological College*, Vol. 23, 1989, pp. 35-44.

[13] J.D. Achenbach, A.K. Gautesen &H. McMaken, *Ray Methods for Waves in Elastic Solids*, Pitman, Boston, 1982.

[14] N.D. Verveiko, Wave propagation in thin viscoelastic layers, *International Applied Mechanics*, Vol. 21, issue 12, pp. 63-67.

[15] M.V. Shitikova, Unsteady vibrations of a plate lying on an elastic isotropic half-space, *Modern Methods of Static and Dynamic Calculation of Structures and Constructions*, *Interuniversity Collection of Scientific Works*, Vol. I, issue 2, 1993, pp. 92-98 [in Russian].

[16] T.Y. Thomas, *Plastic Flow and Fracture in Solids*, Academic Press, New York, 1961.

Contribution of Individual Authors to the Creation of a Scientific Article (Ghostwriting Policy)

The authors equally contributed to the present research, at all stages from the formulation of the problem to the final findings and solution.

Sources of Funding for Research Presented in a Scientific Article or Scientific Article Itself

No funding was received for conducting this study.

Conflict of Interest

The authors have no conflicts of interest to declare.